Growth and characterization of nonpolar, heavily Mn-substituted ZnO films

Q. Shao, P. S. Ku, X. L. Wang, W. F. Cheng, C. W. Leung, and A. Ruotolo

View Online   Export Citation   CrossMark

ARTICLES YOU MAY BE INTERESTED IN

Growth and characterization of nonpolar, heavily Mn-substituted ZnO films

Q. Shao,[1] P. S. Ku,[1] X. L. Wang,[1] W. F. Cheng,[1] C. W. Leung,[2] and A. Ruotolo[1,a)]

[1]*Department of Physics and Materials Science, City University of Hong Kong, Kowloon, Hong Kong SAR, China*
[2]*Department of Applied Physics and Materials Research Centre, The Hong Kong Polytechnic University, Hung Hom, Kowloon, Hong Kong SAR, China*

Eight percent of Mn was successfully diluted into nonpolar ZnO films deposited by pulsed laser deposition on single crystal (100) $SrTiO_3$ substrates. X-ray diffraction patterns and energy-dispersive X-ray spectroscopy confirmed high crystallinity of the films and excluded unintentional magnetic doping. A unique surface domain structure was observed by scanning electron microscope and atomic force microscope, which might play a vital role to strain release induced by lattice mismatch between nonpolar (11–20) ZnO film and (100) $SrTiO_3$ substrate. In addition, the films showed strong ferromagnetism with a large coercivity $H_C \sim 180$ Oe at room temperature. The large magnetic moment is ascribed to carrier-mediated exchange interaction between the Mn ions, where the majority of the carriers are oxygen vacancies. © *2014 AIP Publishing LLC*. [http://dx.doi.org/10.1063/1.4862846]

I. INTRODUCTION

To combine electronics, magnetics, and photonics for next generation multifunctional devices, it is essential to search for magnetic semiconductor materials with independent control of carriers, magnetic moment as well as optical transparency. Transition-metal doped zinc oxide (ZnO) is one of the candidates to meet the above requirements, because this semiconductor is transparent in the visible region due to its wide band-gap (3.3 eV).[1] In the field of spintronics, Mn substituted ZnO is a promising candidate for room temperature diluted magnetic semiconductors (DMS) and has been extensively studied for many practical applications in spin devices.[2] The growth of ferromagnetic semiconductor thin films is undoubtedly of great interest for the emerging spintronic technologies, yet still a challenge in thin film technology because of the low solubility of magnetic elements in the semiconductors.

Generally, owing to the minimal surface energy of (0001) plane, the polar crystal direction $\langle 0001 \rangle$ (*c*-axis) is the priority growth-direction for wurtzite ZnO, even on amorphous substrates.[3] Therefore, there exists a non-vanishing internal electric field polarized along the *c*-axis that thus promotes electrons and holes separation in this direction.[4,5] Such phenomenon is known as quantum confined stark effect (QCSE).[6] This effect compromises the performance of ZnO-based UV optoelectronic devices; therefore the growth of non-polar ZnO is an important topic in thin film technology.[7] Similarly, the possibility to use ferromagnetic ZnO in magneto-optics[8] raises the problem how to grow non-polar magnetic-diluted ZnO.

In this paper, we report on the fabrication of nonpolar $\langle 11-20 \rangle$ 8% Mn substituted ZnO thin films. The films were deposited by pulsed laser deposition (PLD) on (100) $SrTiO_3$ (STO) substrates. The structural, electrical, and magnetic properties of such nonpolar ZnO films were systematically investigated.

II. EXPERIMENT

A single phase dense $Zn_{1-x}Mn_xO$ (x = 0.08) target was prepared via a conventional solid state reaction by mixing and annealing processes.[9,10] During the PLD deposition, a pulsed KrF excimer laser ($\lambda = 247$ nm) with an energy of 300 mJ and a repetition rate of 10 Hz was used. The films were grown on (100) STO substrates in high vacuum (10^{-5} mbar) and at a substrate temperature of 400 °C. As will be discussed later and in agreement with our previous study,[9] these conditions favor high crystal, as well as magnetic order. The crystal structure of the films was investigated by X-ray diffractometry using a Philps X'Pert with Cu Kα radiation source. The stoichiometry of both target and films was checked by energy-dispersive X-ray spectroscopy (EDS). Scanning electron microscopy (SEM) and atomic force microscopy (AFM) were utilized to study the surface morphology. Electrical characterization was carried out by measuring the four-point sheet resistance in magnetic field with a Hall measurement system. The hysteresis loops of the grown films were measured at 300 K by a vibrating sample magnetometer (VSM). The hysteresis loops shown in the following are corrected by subtracting the measured linear contribution of the substrate.

III. RESULTS AND DISCUSSIONS

Fig. 1 shows the XRD pattern of a 100 nm-thick 8% Mn substituted ZnO thin film deposited on single crystal (100) STO substrate. No detectable secondary phases are observed, indicating that all Mn ions are diluted into the host ZnO lattice. The pattern can be indexed by the wurtzite structure of ZnO (JCPDS Card No. 36-1451). While similar films grown under the same conditions on (0001) Al_2O_3 substrates show the diffraction peaks (0002) and (0004) from the ZnO wurtzite structure,[8] in this case, only a strong (11–20) Bragg reflection can be detected. Because of the higher order matching of (11–20) ZnO with (100) STO,[11] the most preferable growth orientation for wurtzite ZnO on single phase

a)E-mail: aruotolo@cityu.edu.hk.
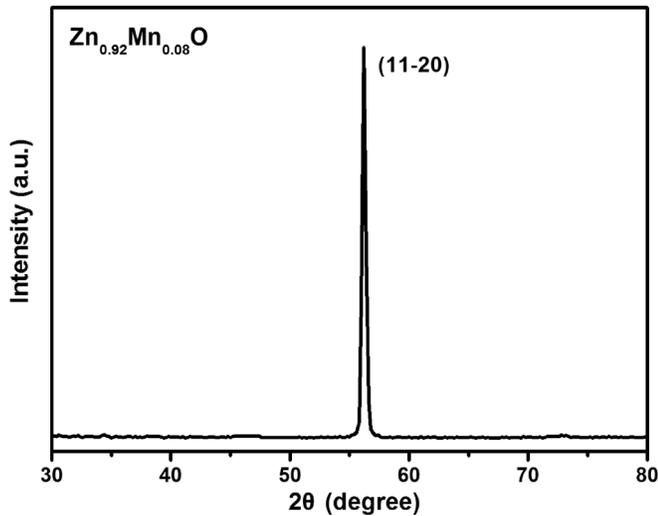
FIG. 1. XRD of a nonpolar 8% Mn substituted ZnO film grown on STO substrate.

(100) STO substrate is $\langle 11{-}20 \rangle$ direction. The peak position in Fig. 1 is at $2\theta = 56.03°$, whereas the same peak for unstrained ZnO is expected to be at $2\theta = 56.60°$. The detected shift of $\Delta\theta = 0.57°$ corresponds to a lattice strain in the (11–20) plane of 0.9%. This small strain induced by the substitution of Mn is consistent with a small difference between the atomic radius of the Mn^{2+} (0.066 nm) and the atomic radius of the Zn^{2+} (0.060 nm). Yet, the lattice mismatch between the (11–20) plane of the film and the (100) substrate is 3% $\left(\frac{\sqrt{3}a_{ZnO} - \sqrt{2}a_{STO}}{\sqrt{2}a_{STO}} \right)$.[11] As the film grows, this large strain must be released, which is usually achieved in

films by randomly introducing grain boundaries. Our morphology analysis (Fig. 2) shows that our system finds a peculiar and ordered manner to release strain.

The SEM image (Fig. 2(a)) shows that the grains grow in two preferential directions, one perpendicular to the other. The tendency of the film to grow along the $\langle 11{-}20 \rangle$ direction (45° from the c-axis) results in a weave pattern. This is confirmed by the AFM scan (Fig. 2(b)). In many applications of ZnO, the surface-area-to-volume ratio is an important factor and much effort is devoted to increase it. In our system, an increase of this ratio is obtained without any further effort but growing the film on (100) STO. From the AFM scan, we can estimate a surface roughness of 32 nm (measured over an area of $10 \times 10\,\mu m^2$) in a film of thickness 100 nm. Moreover, as will be shown in the following, the additional functionality represented by the magnetic order is added.

Given the interest of Mn-substituted ZnO for optoelectronics and spintronics, a complete electrical characterization of the films was carried out by using the Hall effect in van der Pauw geometry. In Fig. 3, we show the resistivity and the carrier density measured in a range of temperatures between 20 and 270 K. The nonpolar film presents *n*-type character with carrier density of $6.93 \times 10^{17}\,cm^{-3}$ at 270 K. It is important to point out that Mn is isovalent to Zn in the wurtzite ZnO, therefore substitution of Zn with Mn does not provide additional electric carriers. On the opposite, oxygen vacancies are double donors and, in films grown under the conditions used in this work, they are the dominant carriers.[9] Since magnetism in dilute magnetic semiconductors is carried mediated, increasing the concentration of oxygen vacancies, as well as that of the magnetic ions, provides a mean to increase magnetic order in the system.
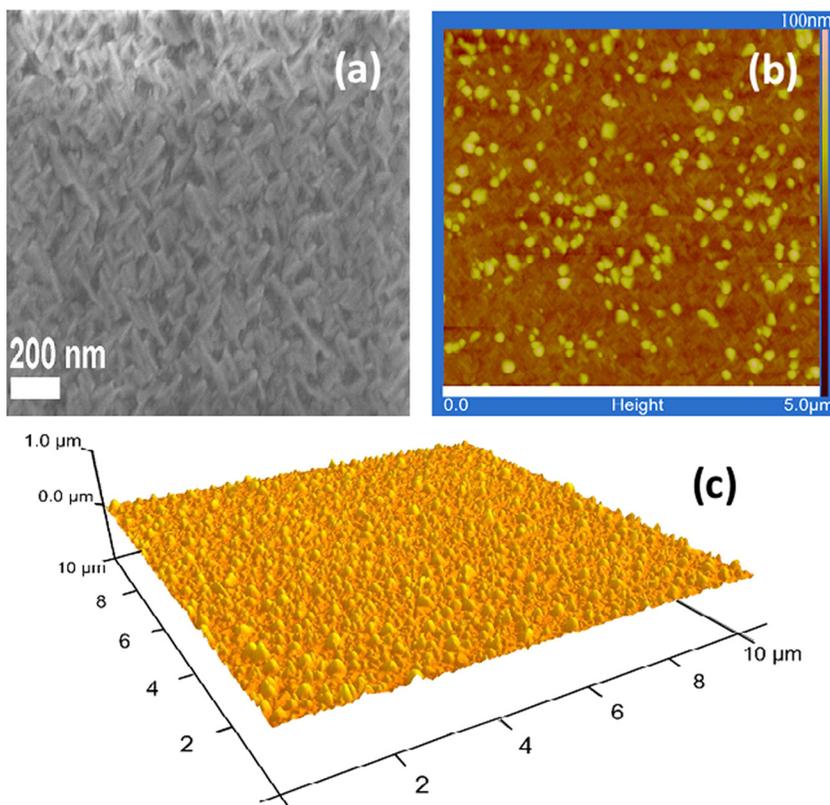
FIG. 2. (a) A typical SEM image of a nonpolar 8% Mn substituted ZnO film grown on STO substrate, (b) $5 \times 5\,\mu m^2$ AFM scan of nonpolar 8% Mn substituted ZnO film, (c) a 3-dimensional AFM scan of the same film.
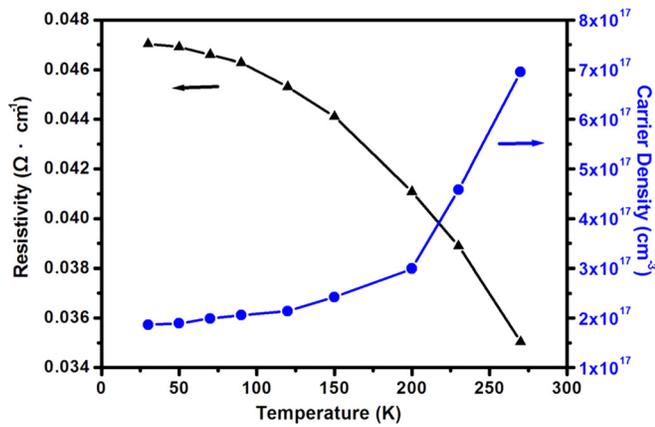
FIG. 3. Temperature dependence of resistivity and carrier density of nonpolar 8% Mn substituted ZnO film grown on STO substrate.
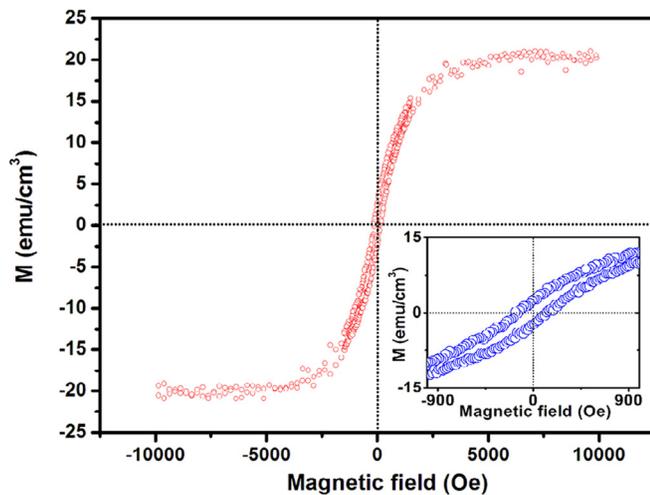
FIG. 4. Magnetic field dependence of the magnetization for the nonpolar 8% Mn substituted ZnO film measured at room temperature; Inset shows the expanded low-field region of the same loop.

Fig. 4 shows the magnetization versus in-plane applied magnetic field at room temperature for a nonpolar Mn substituted ZnO film. Such film displays strong ferromagnetic order with large coercivity $H_C \sim 180$ Oe (see Fig. 4 inset). It should be noticed that Mn substituted ZnO usually shows very small coercivity at room temperature[12] and we have conducted extensive EDX analyses on both the target and the films to exclude the presence of magnetic contamination. The EDX confirm an atomic ratio of Mn:Zn of 8, uniform across the films. In our films, the combination of uniformly diluted Mn and high concentration of oxygen vacancies, assures a magnetic order at room temperature, an important result towards the use of this material in spintronics and magneto-optics.

Let us finally point out that a direct comparison between the magnetic, as well as optical, properties of non-polar and polar ZnO films is not trivial because the non-polar films are nano-structured. In nano-structured films photoluminescence is affected by the large number of surface recombination centres. Moreover, an accurate estimation of the material volume would be required to compare the magnetic moments. Growth of non-polar ZnO compact films remains a challenge for the scientific community.

IV. CONCLUSIONS

We successfully grew nano-structured, nonpolar 8%-Mn-substituted ZnO films by PLD using single phase (100) STO substrates at $400\,°C$ under high vacuum condition. The films show $\langle 11{-}20 \rangle$ growth orientation, as detected by XRD. The EDX measurements excluded the presence of unintentional magnetic dopants. A strong room temperature ferromagnetism measured by VSM shows the potential of this material in the future spintronics and magneto-optics devices.

[1]T. Dietl, H. Ohno, F. Matsukura, J. Cibert, and D. Ferrand, Science **287**, 1019 (2000).
[2]T. Fukumura, Z. Jin, M. Kawasaki, T. Shono, T. Hasegawa, S. Koshihara, and H. Koinuma, Appl. Phys. Lett. **78**, 958 (2001).
[3]H. Funakubo, N. Mizutani, M. Yonetsu, A. Saiki, and K. J. Shinozaki, Electroceramics **4**, 25 (1999).
[4]R. Langer, J. Simon, V. Ortiz, N. T. Pelekanos, A. Barski, R. Ander, and M. Godlewski, Appl. Phys. Lett. **74**, 3827 (1999).
[5]T. Bretagnon, P. Lefebvre, T. Guillet, T. Taliercio, B. Gil, and C. Morhain, Appl. Phys. Lett. **90**, 201912 (2007).
[6]L. F. Zagonel, S. Mazzucco, M. Tence, K. March, R. Bernard, B. Laslier, G. Jacopin, M. Tchernycheva, L. Rigutti, F. H. Julien, R. Songmuang, and M. Kociak, Nano Lett. **11**, 568 (2011).
[7]D. Taïnoff, M. Al-Khalfioui, C. Deparis, B. Vinter, M. Teisseire, C. Morhain, and J.-M. Chauveau, Appl. Phys. Lett. **98**, 131915 (2011).
[8]X. L. Wang, C. Y. Luan, Q. Shao, A. Pruna, C. W. Leung, R. Lortz, J. A. Zapien, and A. Ruotolo, Appl. Phys. Lett. **102**, 102112 (2013).
[9]X. L. Wang, K. H. Lai, and A. Ruotolo, J. Alloys Compd. **542**, 147 (2012).
[10]P. Sharma, A. Gupta, K. V. Rao, F. J. Owens, R. Sharma, R. Ahuja, J. M. O. Guillen, B. Johansson, and G. A. Gehring, Nature Mater. **2**, 673 (2003).
[11]C. H. Jia, Y. H. Chen, X. L. Liu, S. Y. Yang, W. F. Zhang, and Z. G. Wang, Nanoscale Res. Lett. **8**, 23 (2013).
[12]C. Liu, F. Yun, and H. Morkoç, J. Mater. Sci. Mater. Electron. **16**, 555 (2005).